A global cloud detection scheme for high spectral resolution instruments

Lydie Lavanant *, Anthony C. L. Lee **

** Météo-France, Centre de Météorologie Spatiale, BP 147, 22300 Lannion Cedex France*
*** Met Office, Exeter, UK*

Summary

The atmospheric Infrared Sounder (AIRS) was launched in May 2002 on board the AQUA platform and the IASI instrument is foreseen for mid 2006 on board METOP. These high spectral resolution instruments provide several thousands of channels covering the spectral range between 3.7 µm to 15 µm which should permit efficient cloud detection.
Conclusions from a previous study (Lavanant, 2003) indicate that there is no real difficulty to detect and characterize easy clouds (e.g. opaque cold clouds) with classical methods such as the CO_2-slicing or the ECMWF schemes using high resolution sounders alone. However, these schemes are not very effective for clouds with small radiative effects on the observation (e.g. thin semi-transparent clouds, fractional clouds..) having a signal similar to NWP errors.
The main goal of this study is to test different approaches more sensitive to clouds having small radiative effects. We have tested two different cloud detection schemes, the first one based on a PCA approach which takes into account the high frequency cloud information in the sounder spectrum and the second one based on the AVHRR radiances analysis information which will be available at a global scale in the IASI level1c files.
Both schemes have been compared to the full imager cloud mask applied to the co-registered full resolution imager (AVHRR, MODIS). A description of the methods and status on their validation is presented. Finally some suggestions for a robust cloud scheme are given.

Introduction

At the ECMWF 2004 workshop on 'Assimilation of high spectral resolution sounders in NWP', recommendations were made on cloud detection for the IASI level1c processing which point up the need of a day-1 significant reduction of data prior to the NWP assimilation through the use of a NWP-independent cloud detection. Also the need was recognised for a robust and efficient clear detection scheme sensitive to clouds with small radiative effects on the observation of the order of NWP errors. In this study we have tested two approaches which offer promise for improved cloud detection for advanced sounders.

The first method is based on spectral signatures of clouds derived using a Principal Component Analysis. This technique is independent of prior NWP information. In this study it had been validated on AIRS observations collocated with our Meteo-France/CMS MODIS imagery cloud mask.
We do not have a direct broadcast system for the AQUA platform at the CMS, so we obtained level1b MODIS and AIRS data from the NASA/GSFC DAAC web site for only a thirteen days period from 15 to 27 April 2004 in the North Atlantic. The de-archived 46 granules cover different interesting day and night situations with a variety of cloud types. Only sea situations have been processed. The AIRS data are full resolution spectra and the level1b files contain the localization data for all the instruments which avoids re-doing that complex pre-processing. The first period from 15 to 21 April was used as a training period for the computation all the necessary thresholds and the validation is done on the second period from 22 to 27 April.

The second method uses the collocated AVHRR radiance analysis information in terms of clusters provided within the IASI level1c product. The level1c AVHRR clusters are not geophysical information and we have adapted our Meteo-France/CMS AVHRR cloud mask to this information. In this study, the cluster-based cloud mask was compared to the co-registered AVHRR full resolution cloud mask, on the global IASI test dataset provided by EUMETSAT which was generated from a global NOAA17 AVHRR acquisition at full resolution.

MODIS and AVHRR cloud description in sounder FOVs

The MODIS cloud mask used in this study is an adaptation to MODIS of the NWC SAF package with only MODIS channels similar to SEVIRI channels used (LeGléau and Derrien, 2002). Three output parameters are retrieved; the clear/cloud flag, the cloud type and the cloud top temperature and height. For AVHRR, the cloud mask (Lavanant, 2002) follows the same scientific method as the SEVIRI mask. Two output parameters are retrieved, the clear/cloud flag and the cloud type.

Both cloud masks are based on the fact that the spectral behavior of clouds and earth surfaces are different in window channels. The method chosen is a multispectral technique applied every pixel which is efficient in terms of computing time and is relatively easy to adapt. The thresholds are applied to various combinations of channels and depend on the geographical location, on the solar illumination and viewing geometry of the pixel. Thresholds are computed in-line from constant values from experience, from tabulated functions defined off-line through RTTOV simulations, from external data such as NWP forecast fields of land surface temperature and total water vapor content and from climatological atlas of sea surface temperature and albedo.
When a situation is flagged cloudy, a further process is done to determine its cloud type. The input MODIS/AVHRR channels vector goes through a classification tests sequence governed by its illumination (day, night, dawn), with the same philosophy as used previously for computing the thresholds. Ten cloud categories are defined :

- five opaque cloud classes according to their altitude: very low, low, medium, high and very high
- three semi-transparent classes according to their thickness: thick, mean and thin
- one class of semi-transparent clouds above lower clouds
- one fractional clouds class

The accuracy and limits of the cloud mask have extensively been estimated for AVHRR and SEVIRI over several years by the CMS team. See for example (Lavanant, 2002) for AVHRR and www.meteorologie.eu.fr/safnwc for SEVIRI and MODIS.

The processing of the imager pixels mapped inside the sounder FOV is an efficient way to detect small amount of clouds because of its high spatial resolution, to determine the number of cloud layers and the complexity of the situation.
The mapping of MODIS and AIRS is based on their navigation information given in the level1b data and on the scan geometry of the two instruments. An adjustment in line and pixel of the MODIS data in the AIRS FOV is done through the minimization of the differences between AIRS brightness temperatures convoluted on MODIS 32 filter and corresponding MODIS observations averaged on the AIRS ellipse. The adjustment depends on the AIRS scan position. See Lavanant (2003) for more details.
Normally, the correspondence in line and pixel between the IASI level1c and the AVHRR level1b products is directly provided through information in the level1c file. In this study, because the navigation applied to create the IASI level1c and the AVHRR level1b files were different (EUMETSAT navigation for IASI and AAPP navigation for AVHRR), we also applied a technique similar than for MODIS with a minimization between the sum of AVHRR clusters in the IASI FOV and the AVHRR observations averaged on the IASI ellipse. The RMS difference between both was of the order of 0.3-0.5K due mainly to the difference of the ellipse shapes applied.

From the MODIS/AVHRR cloud mask and classification, up to 3 cloud layers are allowed in the sounder ellipse, each of them with a cloud cover, a cloud classification and a top temperature. A situation is declared clear if less than 5% of the imager pixels are cloudy in the ellipse.

PCA-based cloud mask description

This method allows the detection of the clouds through their impact at the highest spatial frequencies within the high spectral resolution sounder spectrum. It is a multiple thresholds cloud discrimination independent of NWP information using cloud-signature eigenvectors. The method has been developed and described by Lee (2001, 2004).

The 'cloudy eigenvectors' are determined on a training dataset by the following method. A Principal Component Analysis is applied to all AIRS spectra discriminated clear with MODIS:

$$S=U\Delta U^t$$

with S the positive-definite covariance matrix of the noise normalized clear AIRS spectra in radiance, U the 'clear-air' eigenvectors and Δ the corresponding eigenvalues. Only the clear-air eigenvectors representative of information above the noise (with eigenvalues larger that 1) are used in the following steps.
Then, the 'clear-air' component of observations using the clear-air PCs are computed for the cloudy profiles of the dataset and subtracted off the observation. A PCA is then applied to the residuals to produce the cloud-signature eigenvectors.
No attempt was made to remove mean spectra when computing covariance matrixes of clear-air spectra or of residuals.

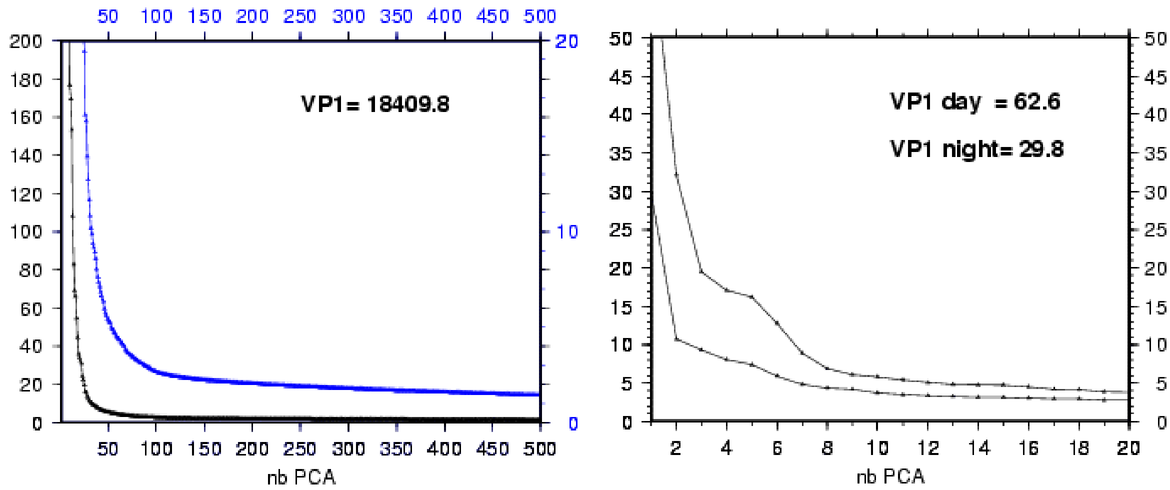

Figures 1: left figure: ranked clear-air eigenvalues, in SNR, all solar illumination. Right figure: ranked cloud-signature eigenvalues, in SNR, differently for day and night situations.

Figures 1 show the ranked clear-air (left figure) and cloud-signature (right figure) eigenvalues in Signal to Noise Ratio: sqrt(Δ) . Cloudy eigenvectors were computed separately for day and night situations. The first clear-air eigenvalue is particularly large because no mean was subtracted. For the cloud-signature eigenvalues, the largest SNR is quite small (62.6 by day and 29.8 by night). The total cloud perturbation SNR is much larger than these values; but a large portion projects onto clear-air eigenvectors, so cannot be used to discriminate clouds. The larger daytime cloud-signature SNR occurs because of the different sunlight reflection characteristics from sea surface and cloud in the near-infrared.

Figures 2 present the first two clear-air and cloudy eigenvectors, all solar illumination. The clear-air eigenvectors show a smooth variation over the spectrum. The cloudy eigenvectors contain a large portion of their energy at high frequency approaching the AIRS sounder spectral resolution. Lee (2001) showed that at IASI spectral resolution, PCA-based techniques could distinguish cloud by examining the edges of spectral lines, especially for water-vapor lines.

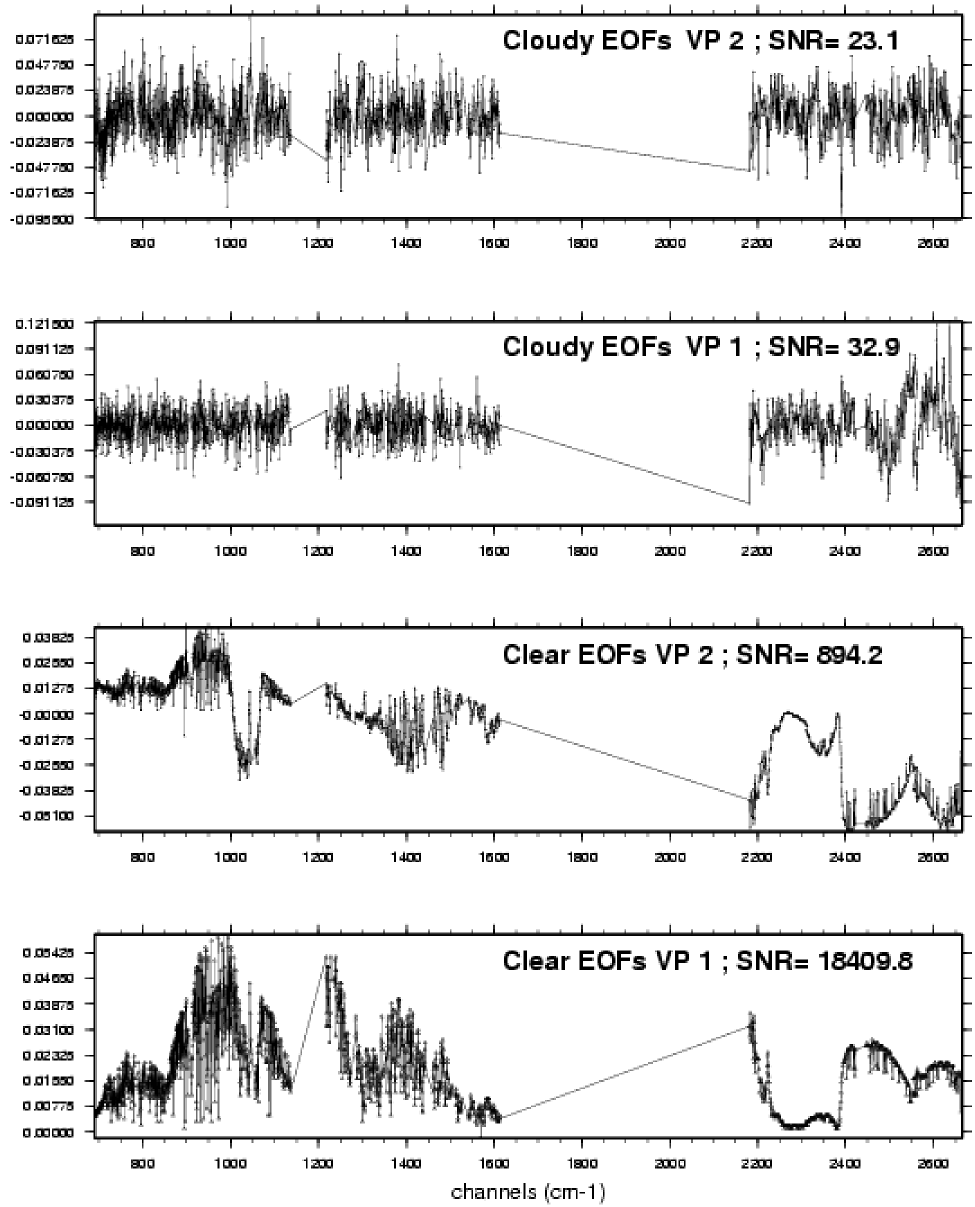

Figures 2: bottom figures: first two clear-air eigenvectors. Upper figures: first two cloud-signature eigenvectors.

In this study, the cloud detection is based on a multiple thresholds discrimination on the scores of the first ten cloud-signature eigenvectors. Figures 3 present on the training dataset the histograms of the scores distribution for the first three cloudy eigenvectors as function of the cloud type given by the collocated MODIS cloud mask. As expected, the score distribution of the clear situations is centered on the zero value with a narrow distribution and an histogram bin-widths of about 1.0. The histograms of the cloudy situations present a one-side distribution for the first eigenvector and mostly a two-side distribution for the others. Also, the histograms of the semi-transparent clouds and of the high opaque clouds are very well separated from the clear histograms whereas the histograms of the clear-sky scenes and of the Very-Low and fractional clouds partly overlap. The MODIS Very-Low classification concerns clouds with a cloud pressure below 850 hPa.

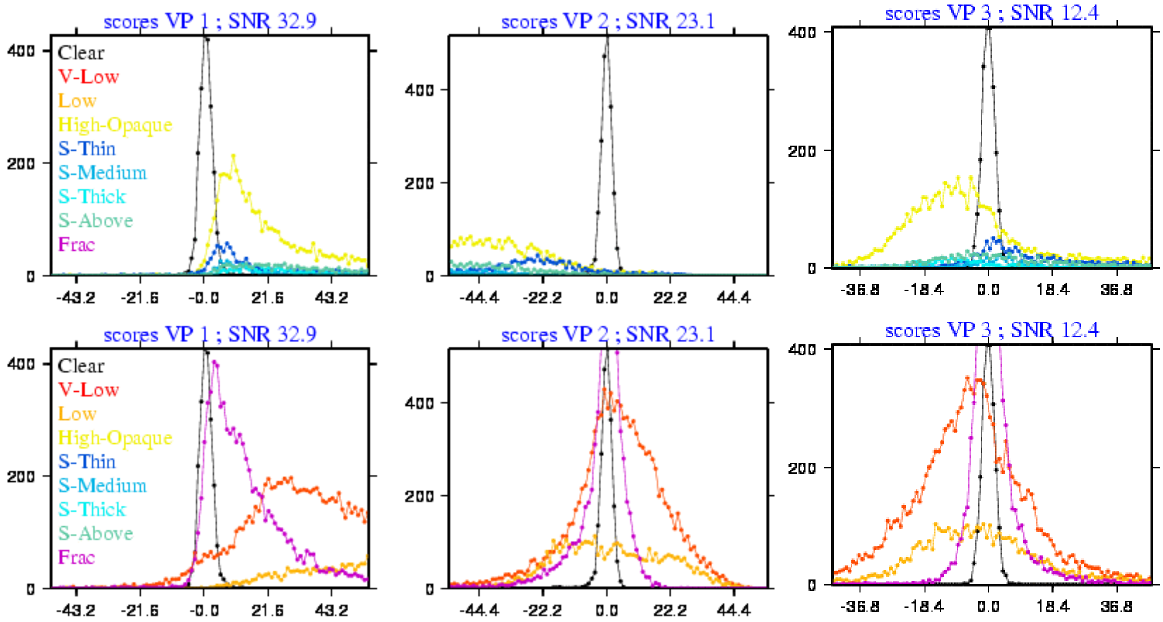

Figures 3: histogram of the scores distribution for the first three cloud-signature eigenvectors from left to right. The upper figures show the distribution for the semi-transparent clouds and high opaque clouds. The bottom figures show the distribution for the opaque very-low to low level clouds plus the fractional clouds. The black curves concern the clear scenes.

In this study, the threshold values have been positioned at the feet of the clear sky scores histograms. A better approach using a thresholds optimizer (e.g. Simplex: Nelder, 1965) by minimizing a penalty function should be used in a future study to maximize the cloud detection for a pre-defined probability of false-rejection of the clear sky situations.

PCA-based cloud mask results

The method has been tested on the second period of the dataset. The training set contains 12 night and 9 day granules whereas the test set contains 13 night and 12 day granules. The cloud detection is a very fast method. It involves the computation of the PC scores on the first ten cloudy-signature eigenvectors for each situation and the situation is declared cloudy if one score is outside the thresholds.

Figures 4 present the agreement of the PCA-based and the co-registered MODIS cloud detections, function of the cloud type. For each type, the left bar shows the agreement on the training set and the right bar on the test set. Results are separated for the night (bottom figure) and the day (upper figure) situations. Getting these results on the test set required to relax the thresholds values by a slight factor of 15% for the night situations but by a larger value of 100% for the daily situations. A possible explanation is that the training set is not well representative of the test set situations. When defining the training set as the odd data and the test set as the even data of the same granules, no relax of the thresholds was needed. A second explanation is that the scores (and the thresholds) are dependent of the environmental conditions, this argument being supported by the fact that we must relax the thresholds by a larger amount for the daytime scenes (e.g.: geometry of the sunlight reflection, possible complexity of shadowing…).

Using the thresholds values as defined previously, and as expected from the day and night cloud-signature first eigenvalue, the PCA-based cloud detection is more efficient for the daytime situations. Between 90 and 95% of the clear sky scenes have been correctly detected. It is easily possible to enlarge this amount by slightly relaxing the thresholds but with as a consequence the degradation of the cloud detection performance mainly for the Very-Low and fractional clouds. More than 90%

(daytime) of the cloudy situations all clouds types merged have been correctly detected. As expected from the scores distribution, the detection of semi-transparent and high opaque clouds is very efficient even for the thin cirrus. The agreement is much better than all other sounder cloud detection methods we tested in previous studies. The method is clearly less efficient for Very-Low level and fractional clouds. Not shown here, most of the cloudy situations false rejected as clear concern situations with small amount of clouds. So far, it is not obvious if we have reached the limits of the method or if we can improve these results with a careful definition of Very-Low signature eigenvectors. This will be studied in more details in a future study.

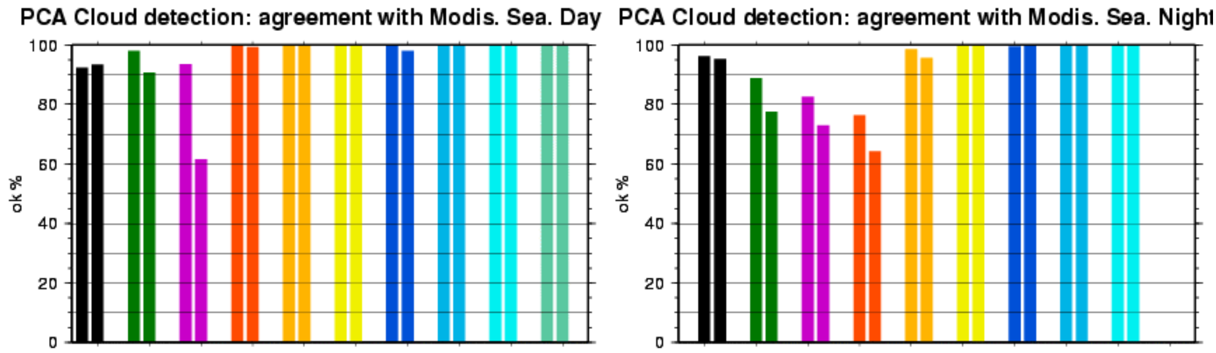

Figures 4: agreement of the PCA-based and the collocated MODIS cloud detections as function of the MODIS cloud type. Colors are the same than on figure 3. Left figure: daytime situations. Number of situations (training/test): clear 1246/818, cloudy 11690/15528. Right figure: nighttime situations. clear 1941/1535, cloudy 18876/18338

Figures 5 present the impact on the radiances of the cloudy situations incorrectly classified as clear with this method. The purpose is to get an estimation of the ability of the PCA-based method to be used alone before the NWP assimilation without any further cloud detection based on NWP information for example. Results are presented for the training dataset, separately for the daytime and nighttime situations. The figures show the bias-corrected departure in RMS between synthetic clear radiances and the observations. The figures only consider the CO_2 part of the spectrum because the bias correction is much difficult elsewhere making the results more difficult to be interpreted. Synthetic clear radiances for the situations determined clear by MODIS are computed using the RTTOV-7 forward model together with the nearest in time and location French ARPEGE NWP atmospheric analysis (back curve) and 6h forecast (blue curve). We notice smaller RMS values for the night conditions probably due to better NWP SST values. Synthetic clear radiances (pink curves) are computed for the cloudy situations false rejected as clear using the nearest NWP analysis. All cloud types are merged.

For the daytime situations, the impact of the incorrectly classified situations is small of the order of 0.1K to 0.15K for the window channels. However, for the nighttime data, the impact of the incorrect classification of cloudy scenes is still important of up to 2K, mainly due to the failure to detect Very-Low level clouds. This means that if the limits of the method are reached for this type of clouds (to be verified), a further cloud discrimination using NWP information during the assimilation step will be needed, mainly for the nighttime data.

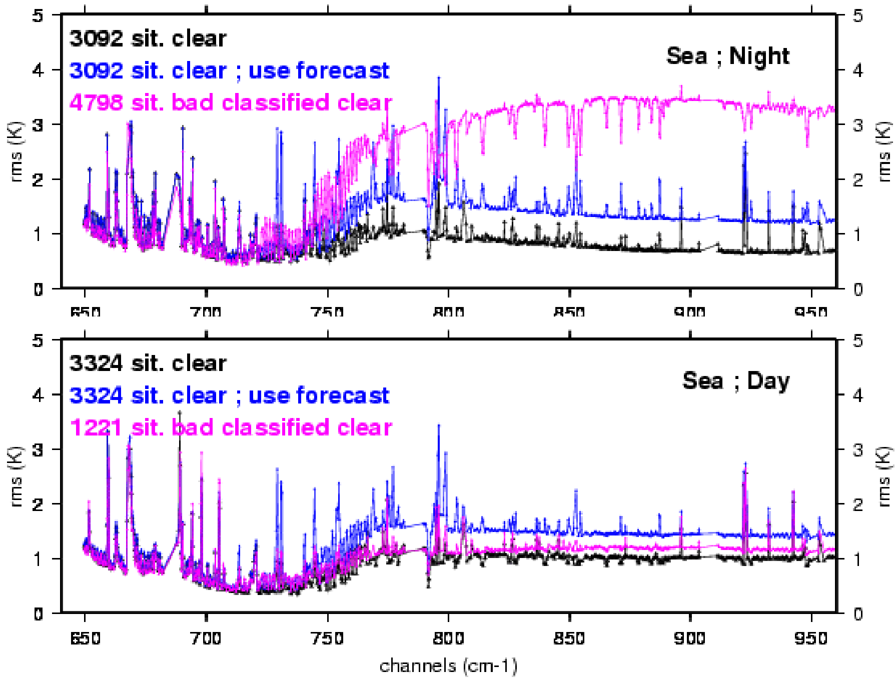

Figures 5: RMS of the bias-corrected departures between RTTOV-7 synthetic clear radiances and observations. Back curves: MODIS clear scenes with the nearest French ARPEGE NWP profile analysis. Blue curves: same but using the nearest 6h forecast instead of the analysis. Pink curves: synthetic clear radiances for the bad classified data (cloudy with MODIS and clear with the PCA-based cloud detection) using the nearest profile analysis.

IASI level1c AVHRR radiances analysis cloud mask

This cloud mask uses the results of the AVHRR radiance analysis method developed by Cayla (2001) and performed within the OPS pre-processing of the EUMETSAT Core Ground Segment (EPS program, 2004). The technique makes a detailed multi-spectral characterization of AVHRR pixels properties and their separation in a limited number of classes. The radiance analysis classes will be part of the description of the IASI level1c product and will be available at a global scale on the GTS and EUMETCast in the BUFR format. The information corresponds to the number of classes actually present in IASI FOV (up to 7) and for each class, the fraction of IASI FOV covered, the mean value of AVHRR channels and the standard deviation of the data which should provides information about compactness of the cluster.

This product was originally developed to describe the IASI sounder FOV in-homogeneity which has to be taken into account for accurately performing retrievals of the inhomogeneous scenes. Indeed, the partition of the FOV between different boundary surfaces (with different surface emissivities) is necessary for the computation of the outgoing radiances. Also the radiance analysis product represents a compression of information compared to the original AVHRR imager data and the reduced volume of data should make easier their exploitation in terms of cloud discrimination in a global NWP assimilation system.

For these two purposes, the geophysical interpretation of the resulting clusters is important for a correct IASI processing in NWP models. In this study, we have adapted our Meteo-France/CMS AVHRR cloud mask (Lavanant, 2002) to the radiance analysis clusters. We have applied the same set of tests to the clusters mean radiances as to the radiances of individual AVHRR pixels. However, the tests based on the local geographical homogeneity characterization applied on the full resolution AVHRR field are not possible and specific efforts are necessary to get equivalent results using the available level1c information. The local geographical homogeneity test is important mainly to detect clouds with small radiative effects on the observation.

The AVHRR cloud mask is dependant on a small number of NWP inputs. Over sea, it makes use of the Total Water Vapor Content if this information is not available from regressions on the collocated AMSU-A observations. Over land, the forecast two-meter air temperature and the TWVC are necessary. Then, the cloud classification is based on the NWP profile temperatures at 500, 700, 850hPa.

In this study, the cluster-based cloud mask is compared to the co-registered AVHRR full resolution cloud mask on the global IASI pre-launch test dataset provided by EUMETSAT. The data was generated from a global NOAA17 AVHRR acquisition at full resolution and allows the comparison on real observations for diverse environment conditions (land, sea, night, dawn, day).

Unfortunately the standard deviation of the clusters is not correctly filled in the EUMETSAT pre-launch dataset and so far new tests based on this information to stand for the local geographical homogeneity were not possible. In later stages we intend to run the OPS software at the CMS to correctly fill this information. In this study we simply applied a threshold test on the difference between the clusters of a same scene for channels 1 and 4. Applied thresholds values are different for land and sea, night and day.

Figure 6 presents the impact of the clustering on the cloud cover for the sea and night situations. A perfect correlation between the cluster-based and the AVHRR full resolution cloud masks should have given the diagonal. The spread of the results around the diagonal is explained by two reasons. First, the radiance analysis is a compression of information and the cloud mask applied to the individual pixels of a same cluster can be differently discriminated clear or cloudy due to the all-or-none thresholds tests, this being more crucial over land and for heterogeneous clouds. Second, the local variance test is different for the two cloud masks. However, even if it is not perfect, there is a good correlation between both results as expected.

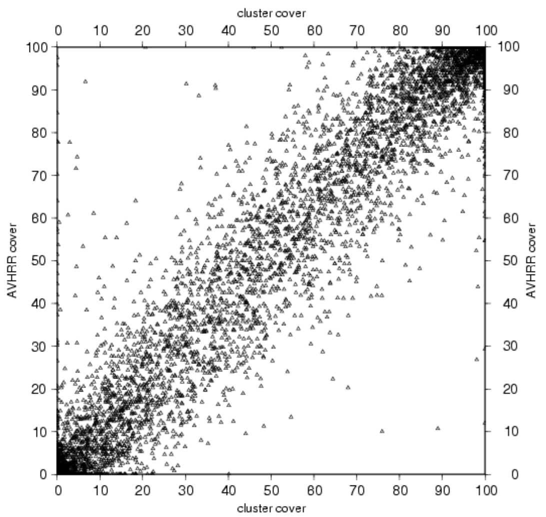

Figures 6: cluster-based and AVHRR full resolution cloud cover comparison. Sea and night situations.

Figures 7 present the cluster-based cloud mask efficiency for the different cloud types and environmental conditions. For all conditions both clear and cloudy (all types merged) scenes detections are efficient with false rejections less than 10% everywhere. In this work a scene is declared clear if less than 5% of AVHRR individual pixels are declared cloudy. The false rejections are partly explained by the dispersion shown on figure 6. The clear detection is better over land because the thresholds of the AVHRR full resolution mask are relaxed compared to the values over sea.

The weakness of the method as applied in this study concerns as always the Very-Low level and fractional clouds and the thin semi-transparent clouds. Thin cirrus seems to be better detected with the

PCA-based cloud mask but of course the situations are different and this will be verified on IASI after the METOP launch.

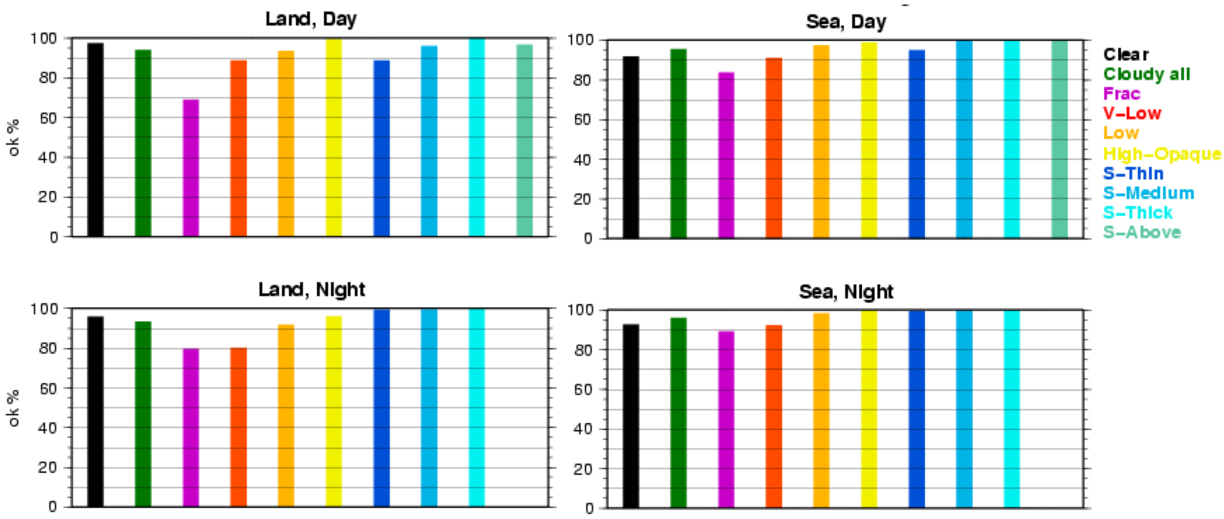

Figures 7: agreement of the IASI AVHRR cluster-based and the collocated AVHRR full resolution cloud discriminations as function of the AVHRR cloud type, on the global EUMETSAT pre-launch test orbit.

Figures 8 show the cloud classification on the land and daytime part of the global orbit of both cloud masks. This example presents the most difficult part of the orbit for getting a good statistical agreement, as seen on figure 7. Some differences exist in the details between both classifications but the synoptic cloud patterns, in cloud detection and type characterization, are correctly detected.

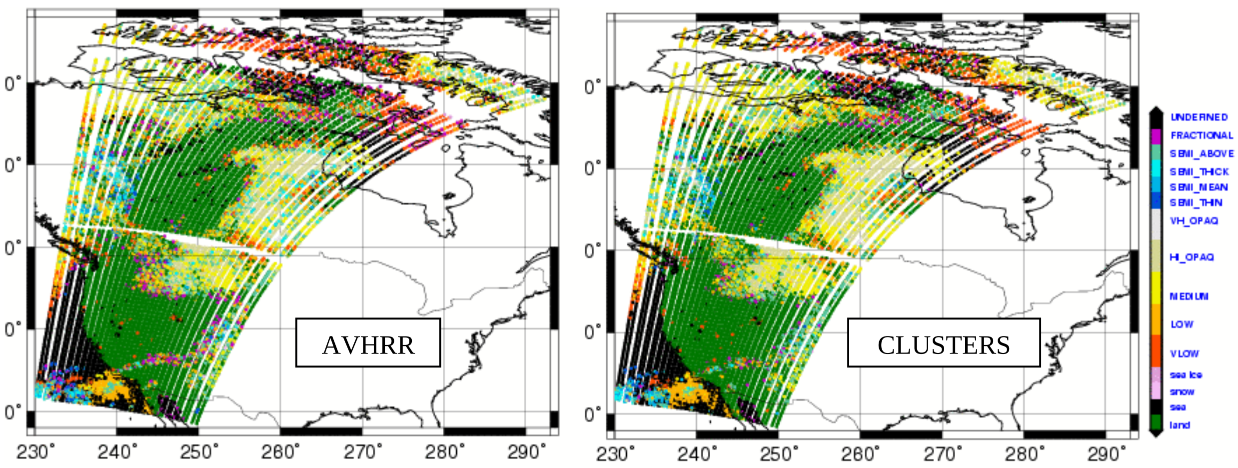

Figures 8: cloud classification comparison for the land and day part of the orbit. Left figure: AVHRR full resolution cloud mask. Right figure: IASI level1c cluster-based cloud mask.

Conclusion

In this work we have tested two new approaches which offer promise for an improved cloud detection in the perspective of the IASI sounder processing. The two methods have been validated on real observations using the collocated imager cloud information.

The PCA-based method allows the detection of the clouds through their impact at the highest spatial frequencies within the high spectral resolution sounder spectrum. The method presents a low sensitivity to the noise through the use of the eigenvectors whose eigenvalues exceed a pre-defined value. This method is independent of any forecast information which makes it easy to be used as a fast pre-selection of scenes before further processing like the NWP assimilation and allows its implementation in a IASI day-2 EUMETSAT CGS pre-processing, with a PCA-based clear/cloudy flag or cloud-signature scores in the day-2 IASI level1c BUFR file.
Results show a general good agreement with the collocated MODIS cloud mask. We got better results for the daytime granules due to the information provided by the sunlight reflection on the clouds. Also, and somewhat surprising, the method is very efficient for semi-transparent clouds even for thin cirrus with a 0% false rejection compared to MODIS for nighttime data on the test dataset.
However, maybe due to the fact that the training dataset was not well representative of the test data or that the PC scores are dependent of the environmental conditions, we had to relax the thresholds for the test data. In this study, the relax factor was experimentally defined, differently for night and day situations and more work is necessary to understand this problem. When fixed, we can expect to improve the thresholds using an optimizer method for maximizing the cloud detection with a pre-defined probability of false-rejection of the clear sky situations. Also, we found that mainly for nighttime data, the sensitivity to clouds was poor near the surface and for fractional clouds. More studies are necessary if we want to get an efficient pre-selection method. We can imagine to define appropriate cloudy eigenvectors for these clouds by differencing the cloudy scenarios in the training dataset.

The second method tested is based on the AVHRR radiance analysis available in the IASI level1c product in terms of radiance clusters. The cloud mask applied on the clusters allows to discriminate between completely and partially covered situations and to provide a cloud type to the scene. Because some NWP input information is necessary mainly over land, the mask can not be used as a pre-selection of scenes like the PCA-based cloud mask. However, it is a good solution to take advantage of the imager information for a global very fast processing. The method could be implemented in the NWP assimilation process in connection with other complementary methods like the ECMWF clear channels selection or the CO_2-slicing cloud top temperature restitution.
The cloud mask applied to the clusters shows a good agreement with the collocated AVHRR full resolution cloud mask, for all clouds except very-low level and fractional clouds. Because the standard deviation associated to each cluster was not correctly filled within the level1c pre-launch test orbit, we have not efficiently substitute the local geographical homogeneity test of the AVHRR full resolution field, useful for the detection of these clouds, by a test based on the heterogeneity of the cluster. We intend to run the OPS software at the CMS on the pre-launch level1b test orbit to correctly fill this information and to define an appropriate test based on it.

References

Antonelli and al, 2004. A principal component noise filter for high spectral resolution infrared measurements . J. of Geophysical Research, **108**, D23102

Cayla, 2001. AVHRR radiances analysis inside IASI FOV's. IA-TN-0000-2092-CNE.

EPS Programme, 2004. IASI level1 Product Format Specification. Technical report EUM.EPS.SYS.SPE.990003

Lavanant, 2002. MAIA v3 AVHRR cloud mask and classification. EUMETSAT documentation.

Lavanant and al, 2003. Use of MODIS imager to help dealing with AIRS cloudy radiances. ITSC13 proceedings.

Lee A., 2001. Assessment of eigenvector-based cloud detection. Met O RSI Branch Working Paper N° 180

Lee, S. Bedford, 2004. Support Study on IASI level1c data compression. EUMETSAT Contract EUM/CO/03/1155/PS.

LeGléau, M. Derrien, 2001. Use of MODIS to enhance the PGE01-02 of SAFNWC/MSG. EUMETSAT documentation.

LeGléau, M. Derrien, 2002. User manual for the PGE01-02-03 of the SAFNWC/MSG: Scientific part. EUMETSAT documentation.

Nelder, R. Mead. Computer J., 7:308-313, 1965.